Approximate solutions for certain bidomain problems in electrocardiography

Peter R. Johnston*
School of Biomolecular and Physical Sciences, Griffith University, Nathan, Queensland, Australia, 4111
(Received 7 March 2008; published 2 October 2008)

The simulation of problems in electrocardiography using the bidomain model for cardiac tissue often creates issues with satisfaction of the boundary conditions required to obtain a solution. Recent studies have proposed approximate methods for solving such problems by satisfying the boundary conditions only approximately. This paper presents an analysis of their approximations using a similar method, but one which ensures that the boundary conditions are satisfied during the whole solution process. Also considered are additional functional forms, used in the approximate solutions, which are more appropriate to specific boundary conditions. The analysis shows that the approximations introduced by Patel and Roth [Phys. Rev. E **72**, 051931 (2005)] generally give accurate results. However, there are certain situations where functional forms based on the geometry of the problem under consideration can give improved approximations. It is also demonstrated that the recent methods are equivalent to different approaches to solving the same problems introduced 20 years earlier.

DOI: 10.1103/PhysRevE.78.041904 PACS number(s): 87.10.Ca, 41.20.−q

I. INTRODUCTION

A study of the electrical behavior of heart tissue can provide insights into the way the electrocardiogram (ECG) (used as a common diagnostic tool by medical practitioners) works. These studies can also explain abnormalities in the ECG on the basis of abnormalities at the cellular level. One such application is the assessment of regions of heart tissue damage following a heart attack. Other applications of these studies are used to influence the design of cardiac pacemakers and defibrillators.

Cardiac tissue can be treated as a passive resistive medium in which Ohm's law governs the relationship between potential difference, tissue resistance, and current flow. However, on a cellular scale conductivity inside a cell differs from conductivity outside the cell. Given that a typical cardiac cell is approximately $100\times10\times10$ μm^3 [1], it would be computationally too expensive to study the electrical behavior of heart tissue on the scale of the human heart. It has also been shown that cardiac tissue exists in sheets of fibers of cardiac cells [2], which also complicates the modeling.

The bidomain model [3] was introduced as a continuum approximation for the electrical properties of cardiac tissue which allows for the fibrous and cellular nature of the tissue. The model consists of an intracellular space (inside the cells) and an extracellular space (outside the cells, but within the cardiac tissue) and allows for anisotropic variations in electrical conductivity in both spaces along and across the direction of the fibers of cardiac cells. Ohm's law is assumed to apply in both of these domains, which are further assumed to coexist spatially.

Over recent years the bidomain model [3] has become the backbone of simulations of many electrocardiographic phenomena. Examples of particular applications are the study of the electrocardiogram itself [4], defibrillation [5], and study of the subendocardial ischemia in cardiac tissue [6–10]. Solutions to the bidomain equations have been achieved via numerical methods [10–13], combined analytical and numerical methods [6–9,14,15], and approximate analytical methods [4,5,16–18].

A conundrum that arises in the formulation of the bidomain model is the following: What are the correct boundary conditions to apply at the interface between the tissue and the surrounding medium (the so-called tissue-bath interface)? Generally, the extracellular tissue potential and the bath potential must satisfy three boundary conditions at the interface, as described in the next section. Through an insightful series of papers, Roth and various co-workers [4,5,16,17] have devised a simple approximation to account for this conundrum and achieve approximate analytical solutions to the bidomain equations. The idea is to simply introduce an exponentially small quantity in the expressions for the potentials, solve for the potentials, and then let the coefficients of the exponential terms tend to zero. This method produces very accurate solutions to the bidomain equations. However, the one small drawback with this idea is that the introduced exponential functions do not necessarily satisfy the boundary conditions on other boundaries in the problem.

In this paper, a modified approximation method, based on introducing what will be called *auxiliary functions*, which satisfy all boundary conditions, is presented. In other words, the functions are based on the geometry of the problem under consideration. It is shown that for defibrillation problems this approximation can be an improvement over previous approximations and can even yield exact solutions.

For cardiac propagation problems the approximations introduced by Patel and Roth [4] are quantified using a method based on choosing auxiliary functions that satisfy the boundary conditions combined with making fewer assumptions during the solution process. A detailed analysis of the approximations shows that the approximate solutions obtained by Patel and Roth are in general equivalent to those obtained by Roth and Wikswo [19] based on a different set of approximating assumptions. Finally, a slightly different formulation is introduced to model subendocardial ischemia, and the so-

*P.Johnston@griffith.edu.au

lutions obtained are compared with previously published solutions [6] and with full numerical solutions.

II. GENERAL METHOD

The bidomain equations that govern the intra- and extracellular potentials in cardiac tissue, ϕ_i and ϕ_e, respectively, are

$$\nabla \cdot (\mathbf{M}_i \nabla \phi_i) = I_m \tag{1}$$

and

$$\nabla \cdot (\mathbf{M}_e \nabla \phi_e) = -I_m, \tag{2}$$

where $\mathbf{M}_i$ and $\mathbf{M}_e$ are the intracellular (i) and extracellular (e) conductivity tensors, respectively, and I_m is the membrane current. Equations (1) and (2) are essentially statements of Ohm's law in the intracellular and extracellular spaces, respectively. The tensors $\mathbf{M}_i$ and $\mathbf{M}_e$ (represented via matrices) reflect the fact that the electrical conductivity of the cardiac tissue is anisotropic, since it is much easier for current to flow along the fibers than across them. Four conductivities are required to describe the behavior of the tissue: intracellular (i) and extracellular (e) conductivities both along the fibers [longitudinal (l)] and across them [transverse (t)]. These conductivities are denoted by σ_i^l, σ_e^l, σ_i^t, and σ_e^t. Note that six conductivities are not required as it is assumed that the conductivities in both transverse directions are equal. Further, if the fibers rotate while moving through the tissue, the tensors also depend on the local fiber directions.

Through the membrane current I_m, the bidomain equations (1) and (2) are coupled, but following Patel and Roth [4], they can be decoupled by defining the transformations

$$\phi_m = \phi_i - \phi_e \quad \text{and} \quad \psi = \frac{\alpha}{1+\alpha}\left(\phi_i + \frac{1}{\alpha}\phi_e\right) \tag{3}$$

with inverse transformations

$$\phi_i = \psi + \frac{1}{1+\alpha}\phi_m \quad \text{and} \quad \phi_e = \psi - \frac{\alpha}{1+\alpha}\phi_m. \tag{4}$$

In these transformations ϕ_m is the transmembrane potential, ψ is an auxiliary potential, and α is an as yet unspecified constant. Using these new potentials, and adding Eqs. (1) and (2), it turns out that

$$\nabla \cdot (\mathbf{M}_i + \mathbf{M}_e) \nabla \psi = -\frac{1}{1+\alpha} \nabla \cdot (\mathbf{M}_i - \alpha \mathbf{M}_e) \nabla \phi_m. \tag{5}$$

For some applications of the bidomain equations it is assumed that ϕ_m [Eq. (3)] can be specified in which case, addition of Eqs. (1) and (2) leads to

$$\nabla \cdot (\mathbf{M}_i + \mathbf{M}_e) \nabla \phi_e = -\nabla \cdot \mathbf{M}_i \nabla \phi_m, \tag{6}$$

where neither the auxiliary potential ψ nor the unspecified constant α are required and the extracellular potential can be obtained directly. In the context of this paper, either Eq. (5) or Eq. (6) will be solved, depending on the example under consideration.

Finally, to complete the formulation of the problem, assume that the tissue is surrounded by a bath of conductivity σ_b, where the bath potential ϕ_b satisfies Laplace's equation

$$\nabla^2 \phi_b = 0. \tag{7}$$

To solve the problem a set of boundary conditions is required. Usually, most of the boundary conditions, which depend on the geometry of the particular problem under consideration, are at the boundaries of the simulation domain, but boundary conditions at the tissue-bath interface are common to all problems.

(1) The extracellular potential is equal to the bath potential,

$$\phi_e = \phi_b. \tag{8}$$

(2) The normal component of the extracellular current density is equal to the normal component of the bath current density,

$$\sigma_e^t \frac{\partial \phi_e}{\partial n} = \sigma_b \frac{\partial \phi_b}{\partial n}. \tag{9}$$

(3) The normal component of the intracellular current density is zero,

$$\sigma_i^t \frac{\partial \phi_i}{\partial n} = 0, \tag{10}$$

where n is the direction perpendicular to the surface, going into the tissue. In terms of the new potentials ϕ_m and ψ these boundary conditions become

$$\psi - \frac{\alpha}{1+\alpha}\phi_m = \phi_b, \tag{11}$$

$$\sigma_e^t (1+\alpha) \frac{\partial \psi}{\partial n} = \sigma_b \frac{\partial \phi_b}{\partial n}, \tag{12}$$

$$\frac{\partial \phi_m}{\partial n} = -(1+\alpha) \frac{\partial \psi}{\partial n}. \tag{13}$$

Alternatively, in the formulation based on ϕ_m and ϕ_e [Eq. (6)], the boundary conditions (8) and (9) remain the same and the boundary condition (10) becomes

$$\frac{\partial \phi_m}{\partial n} = -\frac{\partial \phi_e}{\partial n}. \tag{14}$$

As highlighted by Patel and Roth [4,5], making various assumptions about the form of ϕ_m does not guarantee satisfaction of all three boundary conditions. To overcome this problem for defibrillation problems [5], the authors initiate an iteration scheme by setting

$$\phi_m = A e^{-n/\lambda}, \tag{15}$$

where A is a yet to be determined function, independent of the normal direction n. The form $Ae^{-n/\lambda}$ is used solely to satisfy the boundary conditions at the bath-tissue interface. For cardiac propagation problems [4], the authors write

$$\phi_m = \phi_m^0 + A e^{-n/\lambda}, \tag{16}$$

where ϕ_m^0 presents a planar wave front that is a specific source term and λ can be taken to be the space constant in

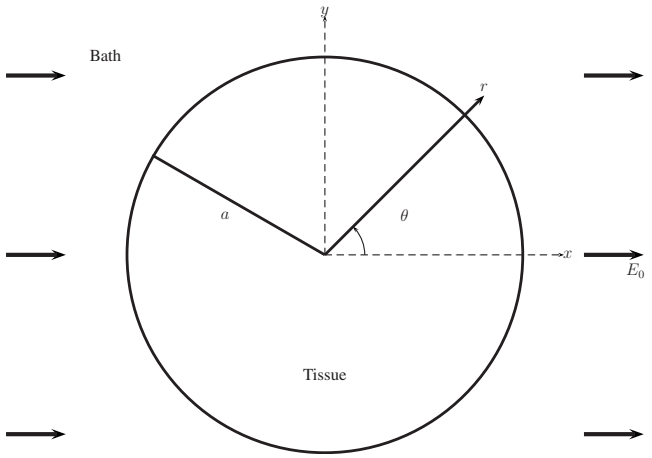

FIG. 1. Defibrillation of a strand of cardiac tissue. A cylindrical strand of radius a placed in a bath with a uniform electric field of strength E_0 applied perpendicular to the strand.

the transverse direction. In order to allow for this additional term and to solve the differential equations, the authors [4] also write

$$\psi = \psi_0 + Be^{-n/\lambda}. \tag{17}$$

In the context of this paper, the exponential function used in (15)–(17) will be referred to as an *auxiliary function*. In what follows other functional forms of the auxiliary function will be considered.

The choice of the exponential function as an auxiliary function is a perfectly logical choice for a tissue of semi-infinite extent in the n direction. In this instance, the exponential function decays to zero as n increases and will decay rapidly when λ is small. However, if the tissue is of finite extent in the n direction then the exponential function may not satisfy other boundary conditions required by the physical situation, and other forms of the auxiliary function should be considered, typically hyperbolic functions or modified Bessel functions. Although these functions exhibit similar behaviors to the exponential function, they satisfy the necessary boundary conditions at other boundaries in the problem. The degree to which these functions mimic the behavior of exponential functions depends on the parameter λ, so if the scale over which the problem is defined is large compared to λ, the choice of an auxiliary function that is a simple exponential function is perfectly adequate. However, if the scale is of the order of λ or smaller, then a more appropriate auxiliary function should be chosen.

The best way to highlight this approach is via a number of examples.

III. EXAMPLE 1: CYLINDRICAL STRAND IN A UNIFORM ELECTRIC FIELD

Consider a cylindrical strand of cardiac tissue of radius a in an electric field E_0 perpendicular to the strand (Fig. 1). It is assumed that the fibers lie along the strand (into the plane of Fig. 1) and that end effects can be ignored, meaning that the potentials are independent of z. Further, assume that the intracellular and extracellular conductivities in the transverse directions are equal, that is, $\sigma_i^x = \sigma_i^y = \sigma_i^t$ and $\sigma_e^x = \sigma_e^y = \sigma_e^t$. Due to these assumptions, the zeroth term in Patel and Roth's iteration scheme [5] is the full solution to the problem. Hence, the governing equations for ψ and ϕ_b in a cylindrical coordinate system are

$$\frac{1}{r}\frac{\partial}{\partial r}\left(r\frac{\partial \psi}{\partial r}\right) + \frac{1}{r^2}\frac{\partial^2 \psi}{\partial \theta^2} = 0 \tag{18}$$

and

$$\frac{1}{r}\frac{\partial}{\partial r}\left(r\frac{\partial \phi_b}{\partial r}\right) + \frac{1}{r^2}\frac{\partial^2 \phi_b}{\partial \theta^2} = 0, \tag{19}$$

subject to the boundary conditions (11)–(13). At large values of r, the electric field is uniform in the x direction, so ϕ_b becomes $-E_0 r \cos\theta$. Therefore, the general solutions to (18) and (19) can be written as

$$\psi = Br\cos\theta,$$

$$\phi_b = -E_0 r\cos\theta + \frac{C}{r}\cos\theta,$$

where B and C are unknown constants.

Patel and Roth [5] suggest that the transmembrane potential ϕ_m should fall exponentially with depth below the surface. However, from a physical standpoint, it is also required that $\phi_m = 0$ at $r=0$, so a better choice for the auxiliary function would involve modified Bessel functions. Hence, the form of ϕ_m is chosen to be

$$\phi_m = A\cos\theta\frac{I_1(r/\lambda)}{I_1(a/\lambda)}, \tag{20}$$

where I_1 is a modified Bessel function of the first kind of order 1. This choice of auxiliary function exhibits exponential decay with depth below the surface, takes the value $A\cos\theta$ at the surface and is zero when $r=0$. Substituting the approximation (20) into the boundary condition (13) gives

$$A = -(1+\alpha)\lambda\frac{I_1(a/\lambda)}{I_1'(a/\lambda)}\left.\frac{\partial \psi}{\partial r}\right|_{r=a}. \tag{21}$$

Further, substituting for A from (21) in the boundary condition (11) gives the new mixed boundary condition at $r=a$,

$$\phi_b = \psi + \lambda\alpha\frac{I_1(a/\lambda)}{I_1'(a/\lambda)}\frac{\partial \psi}{\partial r}. \tag{22}$$

If it is assumed that $\psi = \phi_b$ at $r=a$ (following Patel and Roth [5]), it follows that

$$A = 2E_0\lambda(1+\alpha)\frac{I_1(a/\lambda)}{I_1'(a/\lambda)}\frac{\sigma_b/\sigma_T}{1+\sigma_b/\sigma_T},$$

$$B = -2E_0\left(\frac{\sigma_b/\sigma_T}{1+\sigma_b/\sigma_T}\right),$$

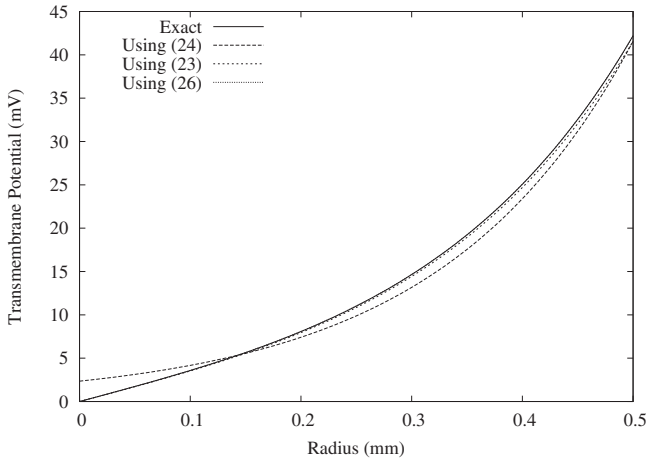

FIG. 2. Various approximate solutions and the exact solution for the transmembrane potentials plotted against radial distance for a cylindrical strand of cardiac tissue with $a=0.5$ mm, $\alpha=0.25$, $\lambda=0.174$ mm, $\sigma_T=0.0931$ S/m, $\sigma_b=2$ S/m and $E_0=100$ V/m.

$$C = E_0 a^2 \left(\frac{1 - \sigma_b/\sigma_T}{1 + \sigma_b/\sigma_T} \right),$$

giving

$$\phi_m = 2E_0\lambda(1+\alpha)\frac{\sigma_b/\sigma_T}{1+\sigma_b/\sigma_T}\frac{I_1(r/\lambda)}{I_1'(a/\lambda)}\cos\theta, \tag{23}$$

where $\alpha=\sigma_i^l/\sigma_e^l$ and $\sigma_T=\sigma_i^l+\sigma_e^l$.

Figure 2 shows a plot of the transmembrane potential ϕ_m [Eq. (23)] for a thin strand of cardiac tissue (of radius 0.5 mm) along $\theta=0$, as well as a plot of the expression for ϕ_m obtained by Patel and Roth [5],

$$\phi_m = 2E_0\lambda(1+\alpha)\frac{\sigma_b/\sigma_T}{1+\sigma_b/\sigma_T}e^{-(a-r)/\lambda}\cos\theta, \tag{24}$$

and the exact expression for ϕ_m [4],

$$\phi_m = 2aE_0\frac{1+\alpha}{\alpha} \times \frac{I_1(r/\lambda)}{I_1(a/\lambda)}\frac{1}{1+a/\alpha\lambda(1+\sigma_T/\sigma_b)I_1'(a/\lambda)/I_1(a/\lambda)}\cos\theta. \tag{25}$$

(Parameter values are given in the figure caption.) The figure shows that the new expression for ϕ_m (23) more closely matches the exact solution. In particular, there is a very good match for the inner 10% of the radius of the strand. This is opposed to the approximate solution (24), which shows its greatest deviation in this inner region. It is interesting to observe that both approximate solutions (23) and (24) tend to the same value at $r=a$, which is slightly lower than the exact value. This is presumably a result of the fact that both are trying to satisfy the approximate boundary condition $\psi=\phi_b$ at $r=a$.

The approximate solution (23) can be improved by actually applying the boundary condition (22). After some algebra it follows that

$$A = 2aE_0\frac{1+\alpha}{\alpha}\frac{1}{1+a/\alpha\lambda(1+\sigma_T/\sigma_b)I_1'(a/\lambda)/I_1(a/\lambda)}, \tag{26}$$

which, in turn, yields the exact solution to the problem. Hence, use of an auxiliary function for the solution based on physical insights into the problem under consideration can yield an exact solution to the problem when no further approximations are made during the solution process.

IV. APPROXIMATIONS RECONSIDERED

Before consideration of an electrocardiographic-type example with a propagation wave front, it is worthwhile to reexamine the approximations of Patel and Roth [4]. The idea with such problems is to solve the governing equations (5) and (7) subject to the boundary conditions (11)–(13) with a specified ϕ_m. As discussed above, Patel and Roth [4] introduce the forms (16) and (17) and substitute these into Eq. (5) to obtain

$$\nabla\cdot(\mathbf{M}_i+\mathbf{M}_e)\nabla\psi_0 = 0 \tag{27}$$

subject to the boundary conditions

$$-\frac{\alpha}{1+\alpha}\phi_m^0 + \psi_0 = \phi_b \tag{28}$$

and

$$\sigma_T\frac{\partial\psi_0}{\partial n} = \sigma_b\frac{\partial\phi_b}{\partial n} \tag{29}$$

at the bath-tissue interface.

These equations are derived under the assumption that propagation is along the fiber direction and that $\alpha=\sigma_i^l/\sigma_e^l$. It is also assumed that the coefficients A and B in Eqs. (16) and (17) can be ignored since both A and B tend to zero as $\lambda\to 0$. Hence, in order to obtain approximate solutions to Eqs. (1), (2), and (7) subject to the boundary conditions (8)–(10) at the bath-tissue interface (as well as other geometry-specific boundary conditions), one simply has to solve Eqs. (27) and (7) subject to the boundary conditions (28) and (29) to yield ψ_0 and ϕ_b.

Now examine these approximations in terms of the original functions ϕ_i and ϕ_e. From Eq. (4) it follows that

$$\phi_i = \psi + \frac{1}{1+\alpha}\phi_m = \psi_0 + \frac{1}{1+\alpha}\phi_m^0, \tag{30}$$

since the coefficients A and B have been ignored. In turn, it also follows that

$$\frac{\partial\phi_i}{\partial n} = \frac{\partial\psi_0}{\partial n}, \tag{31}$$

as ϕ_m^0 is independent of depth in the n direction. It further follows that $\partial\phi_i/\partial n\neq 0$ since equality is obtained only when the coefficients A and B are included, regardless of their magnitude. Further, by a similar argument it can also be shown that

$$\frac{\partial \phi_e}{\partial n} = \frac{\partial \psi_0}{\partial n}. \tag{32}$$

With these approximations, consider the boundary condition (29):

$$\sigma_b \frac{\partial \phi_b}{\partial n} = \sigma_T \frac{\partial \psi_0}{\partial n} = (\sigma_i^t + \sigma_e^t)\frac{\partial \psi_0}{\partial n}$$

$$= \sigma_i^t \frac{\partial \psi_0}{\partial n} + \sigma_e^t \frac{\partial \psi_0}{\partial n} = \sigma_i^t \frac{\partial \phi_i}{\partial n} + \sigma_e^t \frac{\partial \phi_e}{\partial n}. \tag{33}$$

Hence, the approximate solutions ϕ_0 and ϕ_b do not lead to solutions ϕ_i and ϕ_e that satisfy the boundary conditions (9) and (10), but to solutions that satisfy the weaker condition (33).

The above argument justifies the observation by Patel and Roth [4] that their approximate solutions obtained for propagation along a cylindrical fiber are equivalent to those derived by Roth and Wikswo [19], who assumed that ϕ_m was independent of depth and did not enforce the boundary condition (10), replacing the boundary condition (9) with the condition (33). Moreover, the above argument demonstrates that this observation is true for propagation in any geometry.

To summarize, in order to use the approximation method of Patel and Roth [4] and satisfy the boundary conditions (9) and (10), it is necessary to include the coefficients A and B in Eqs. (16) and (17) both during the solution process and in the final solutions. Ignoring the coefficients A and B results in a solution that satisfies the boundary condition (33), which has been shown [20] to be an inappropriate boundary condition for use with the bidomain equations. Even though these coefficients have been shown to be very small in magnitude, their inclusion is necessary to solve the governing equations and boundary conditions correctly.

V. EXAMPLE 2: TWO-DIMENSIONAL TISSUE ANALYSIS

In light of the above discussion, the two-dimensional analysis of Patel and Roth [4] will be reexamined. Consider a slab of tissue in the region $z<0$, which is perfused by a bath ($z>0$). Assume that a planar wave front propagates in the x direction (parallel to the fibers) with the wave front being independent of y (Fig. 3). Using the approximations (16) and (17) and previously mentioned assumptions, the governing equations are

$$\frac{\partial^2 \phi_b}{\partial x^2} + \frac{\partial^2 \phi_b}{\partial z^2} = 0 \tag{34}$$

and

$$\sigma_L \frac{\partial^2 \psi_0}{\partial x^2} + \sigma_T \frac{\partial^2 \psi_0}{\partial z^2} = 0, \tag{35}$$

where $\sigma_L = \sigma_i^l + \sigma_e^l$.

Patel and Roth [4] show that (in the notation of this paper)

$$A = \frac{\sigma_e^t + \sigma_i^t}{\sigma_e^t} \lambda \left. \frac{\partial \psi_0}{\partial z} \right|_{z=0} \tag{36}$$

and

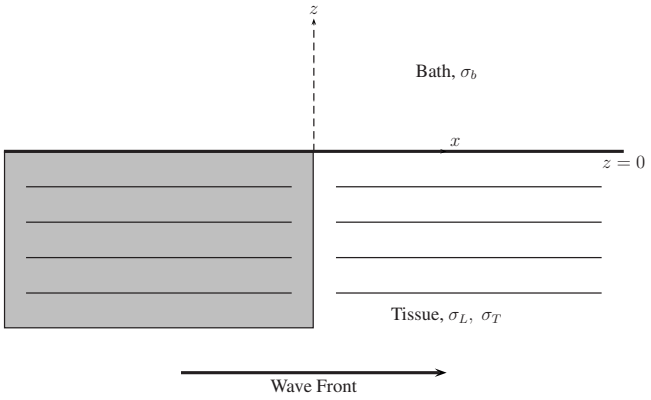

FIG. 3. A semi-infinite block of cardiac tissue, perfused by a bath of conductivity σ_b containing a planar wave front propagating in the x direction. The horizontal lines represent the fiber directions and the shaded area represents the action potential.

$$B = -\frac{\sigma_i^t - \alpha \sigma_e^t}{(1+\alpha)\sigma_e^t} \lambda \left. \frac{\partial \psi_0}{\partial z} \right|_{z=0}, \tag{37}$$

where $\alpha = \sigma_i^l / \sigma_e^l$.

Substitution of the expressions (16) and (17) into the boundary conditions (11) and (12) gives the following boundary conditions at $z=0$:

$$\psi_0 - \frac{\alpha}{1+\alpha}\phi_m^0 - \lambda \frac{\sigma_i^t}{\sigma_e^t}\frac{\partial \psi_0}{\partial z} = \phi_b \tag{38}$$

and

$$\sigma_T \frac{\partial \psi_0}{\partial z} = \sigma_b \frac{\partial \phi_b}{\partial z}. \tag{39}$$

Assuming that ϕ_m^0 varies sinusoidally in the x direction with spatial frequency k (i.e., $\phi_m^0 = V_0 \sin kx$), the solutions of (34) and (35) are then

$$\phi_b(x,y) = Ce^{-kz} \sin kx \tag{40}$$

and

$$\psi_0(x,z) = De^{\delta kz} \sin kx, \tag{41}$$

where $\delta = \sqrt{\sigma_L / \sigma_T}$. Next, substitution of (40) and (41) into the boundary conditions (38) and (39) gives

$$C = -\frac{\alpha}{1+\alpha} V_0 \frac{\sqrt{\sigma_L \sigma_T}}{\sigma_b} \frac{1}{1 + \sqrt{\sigma_L \sigma_T}/\sigma_b + \lambda k (\sigma_i^l/\sigma_e^l)\sqrt{\sigma_L/\sigma_T}}. \tag{42}$$

and

$$D = \frac{\alpha}{1+\alpha} V_0 \frac{1}{1 + \sqrt{\sigma_L \sigma_T}/\sigma_b + \lambda k (\sigma_i^l/\sigma_e^l)\sqrt{\sigma_L/\sigma_T}}. \tag{43}$$

When compared with the corresponding coefficients obtained by Patel and Roth [4], both these coefficients contain a small correction factor that depends on the product λk. The final solution for ψ is then

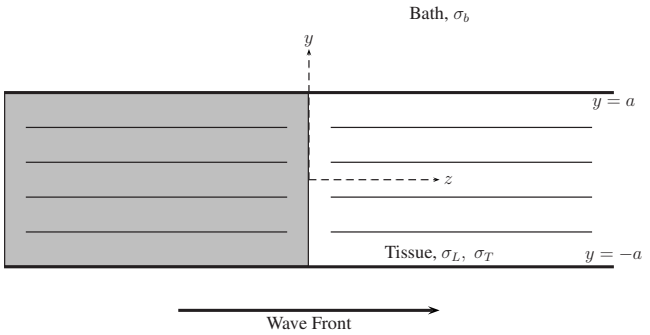

FIG. 4. A slab of cardiac tissue of thickness $2a$, perfused by a bath of conductivity σ_b on both sides (for $|y|>a$) with planar wave front propagating along the z direction. The format is the same as in Fig. 3.

$$\psi = \frac{\alpha}{1+\alpha} V_0 \frac{1}{1+\sqrt{\sigma_L \sigma_T}/\sigma_b + \lambda k (\sigma_i^l/\sigma_e^l)\sqrt{\sigma_L/\sigma_T}} \sin kx \times \left(e^{\delta k z} + \lambda k \frac{\sigma_i^t - \alpha \sigma_e^t}{(1+\alpha)\sigma_e^t} \sqrt{\frac{\sigma_L}{\sigma_T}} e^{z/\lambda} \right). \quad (44)$$

As the product λk tends to zero, the solution (44) tends to the solution obtained by Patel and Roth [4].

In order to quantify the difference between the solution (44) and the solution of Patel and Roth (which will be labeled ψ_{PR}), consider a comparison of the coefficient of $\sin kx$ at the surface $z=0$ as a function of k. Using the set of parameters given in [4], $\sigma_i^l=0.2$ S/m, $\sigma_e^l=0.2$ S/m, $\sigma_i^t=0.02$ S/m, $\sigma_e^t=0.08$ S/m and $\sigma_b=1.0$ S/m, and defining the relative error as $|(\psi-\psi_{\mathrm{PR}})/\psi_{\mathrm{PR}}|$, it can be shown via a simple asymptotic argument for small values of λk that the relative error is given by approximately $\frac{5}{3}\lambda k$. So, for example, if $\lambda k=0.01$, then the relative error is of the order of 0.0167.

The above argument shows that, for this example, solution of the equations with a method that makes fewer approximations does not significantly improve the accuracy of the solutions obtained by Patel and Roth [4]. The argument does, however, quantify the effects of the approximations made by Patel and Roth.

VI. EXAMPLE 3: PLANAR SLAB MODEL

Consider a slab of cardiac tissue of thickness $2a$ with parallel fibers aligned along the z direction. An action potential propagates in the z direction, which is independent of x, with the y direction being parallel to the tissue surface (Fig. 4). The tissue is perfused by a bath for $|y|>a$, and so the problem is symmetric about the plane $y=0$. The governing equations are (5) and (7), which can be written for this example as

$$\sigma_T \frac{\partial^2 \psi}{\partial y^2} + \sigma_L \frac{\partial^2 \psi}{\partial z^2} = 0 \quad (45)$$

and

$$\frac{\partial^2 \phi_b}{\partial y^2} + \frac{\partial^2 \phi_b}{\partial z^2} = 0. \quad (46)$$

In terms of the original variables ϕ_i and ϕ_e, the boundary conditions necessary to solve this problem are given by (8)–(10) at $y=a$, along with, at $y=0$,

$$\frac{\partial \phi_i}{\partial y} = \frac{\partial \phi_e}{\partial y} = 0. \quad (47)$$

This last condition implies that at $y=0$

$$\frac{\partial \phi_m}{\partial y} = \frac{\partial \psi}{\partial y} = 0. \quad (48)$$

To solve this problem Patel and Roth [4] write

$$\phi_m = \phi_m^0 + A e^{-(y-a)/\lambda}$$

and

$$\psi = \psi^0 + B e^{-(y-a)/\lambda},$$

using the exponential function as the auxiliary function. However, this choice of ϕ_m and ψ violates the boundary condition (48), since ϕ_m^0 is assumed to be a planar wave front with no variation perpendicular to the surface.

In order to overcome this problem, it is more correct to choose an auxiliary function based on the hyperbolic cosine, writing

$$\phi_m = \phi_m^0 + A \frac{\cosh(y/\lambda)}{\cosh(a/\lambda)} \quad (49)$$

and

$$\psi = \psi^0 + B \frac{\cosh(y/\lambda)}{\cosh(a/\lambda)}. \quad (50)$$

This choice of the auxiliary function takes on the value 1 at the bath-tissue interface at $y=a$ and ensures that the boundary conditions (48) are satisfied.

To find a relationship between A and B, substitute (49) and (50) into (5) and consider only derivatives perpendicular to the surface. After some algebra, this yields

$$B = -\frac{1}{1+\alpha} \frac{\sigma_i^t - \alpha \sigma_e^t}{\sigma_i^t + \sigma_e^t} A \quad (51)$$

as obtained by Patel and Roth [4]. Next, use of the boundary condition (13) gives

$$A = -\lambda \frac{\partial \psi_0}{\partial y} \frac{\sigma_i^t + \sigma_e^t}{\sigma_e^t} \coth(a/\lambda), \quad (52)$$

which leads to

$$B = \lambda \frac{\partial \psi_0}{\partial y} \frac{\sigma_i^t - \alpha \sigma_e^t}{\sigma_e^t (1+\alpha)} \coth(a/\lambda). \quad (53)$$

Finally, on substituting (52) and (53) into the boundary conditions (11) and (12), we obtain the following boundary conditions at $y=a$ for ψ_0 and ϕ_b:

$$\phi_b = \psi_0 - \frac{\alpha}{1+\alpha}\phi_m^0 + \lambda\frac{\partial\psi_0}{\partial y}\frac{\sigma_i^t}{\sigma_e^t}\coth(a/\lambda) \tag{54}$$

and

$$\sigma_T\frac{\partial\psi_0}{\partial y} = \sigma_b\frac{\partial\phi_b}{\partial y}, \tag{55}$$

where the assumption that λ is small compared to the spatial scale has been ignored. The boundary condition (55) is identical to that obtained by Patel and Roth [4], but (54) is a new mixed boundary condition. Clearly letting $\lambda\to 0$ results in the boundary condition obtained by Patel and Roth.

The task now is to solve Eqs. (45) and (46). Substitution of the approximations (49) and (50) into (45) and (46) gives

$$\sigma_T\frac{\partial^2\psi_0}{\partial y^2} + \sigma_L\frac{\partial^2\psi_0}{\partial z^2} = 0 \tag{56}$$

and

$$\frac{\partial^2\phi_b}{\partial y^2} + \frac{\partial^2\phi_b}{\partial z^2} = 0. \tag{57}$$

These two equations are solved subject to the boundary conditions (12) and (55). As discussed by Patel and Roth [4], the equations are best solved in Fourier transform space, and yield

$$\widehat{\psi_0}(y,k) = \frac{\alpha}{1+\alpha}\frac{\cosh(\delta k y)}{\beta(|k|,a,\delta,\lambda)\cosh(\delta k a)}\widehat{\phi_m^0}(k) \tag{58}$$

and

$$\hat{\phi}_b(y,k) = -\frac{\alpha}{1+\alpha}\frac{\sigma_T}{\sigma_b}\delta\frac{e^{-k(y-a)}}{\beta(|k|,a,\delta,\lambda)}\tanh(\delta k a)\widehat{\phi_m^0}(k), \tag{59}$$

where

$$\widehat{\phi_m^0}(k) = \int_{-\infty}^{\infty}\phi_m^0(z)e^{ikz}dz$$

and

$$\beta(|k|,a,\delta,\lambda) = 1 + \frac{\sigma_T}{\sigma_b}\delta\tanh(\delta k a) + \lambda\delta k\tanh(\delta k a)\coth a/\lambda.$$

Substitution of Eqs. (58) and (53) into a transformed version of Eq. (50) gives

$$\hat{\psi}(y,k) = \frac{\alpha}{1+\alpha}\frac{1}{\beta(|k|,a,\delta,\lambda)}\frac{\cosh(\delta k y)}{\cosh(\delta k a)} \times\left(1+\lambda\delta k\tanh(\delta k y)\frac{\cosh(y/\lambda)}{\sinh(a/\lambda)}\frac{\sigma_i^t-\alpha\sigma_e^t}{(1+\alpha)\sigma_e^t}\right). \tag{60}$$

Taking the limit as $\lambda\to 0$ gives the same solution as obtained previously [4].

To contrast the difference between the solution (60) obtained above and that obtained by Patel and Roth [4], consider the relative error as defined above, but in terms of transformed functions. Figure 5 shows the relative error on the bath-tissue interface, $y=a$, against frequency k for values of a of 1.5 mm (typical of the thickness of the atrial wall) and 5 mm (typical of the thickness of the ventricular wall) using the same conductivity values as above. The figure shows that the errors increase as k increases, but for lower frequencies they are generally less than 0.005. It is interesting to note that the errors are larger for the ventricular wall ($a=5$ mm) than for the atrial wall ($a=1.5$ mm). Again, as in the previous example, it appears that the extra effort expended in using solutions that satisfy the boundary conditions exactly is not justified.

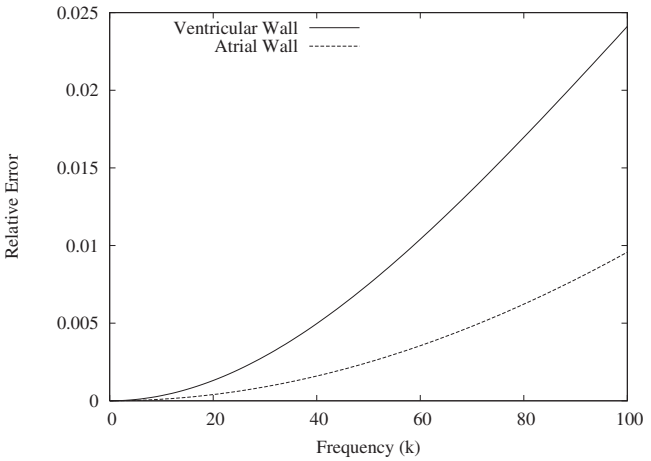

FIG. 5. Relative error between surface potentials for two approximate solutions for propagation in a slab of cardiac tissue of finite thickness.

VII. EXAMPLE 4: MODELING SUBENDOCARDIAL ISCHEMIA DURING THE ST SEGMENT

This example studies the electric field produced with cardiac tissue when there is a region of ischemia (damaged tissue) present. Simulations are performed during the ST segment of the ECG where the entire heart is depolarized and assumptions of steady state electric fields can be exploited.

Consider a slab of cardiac tissue, infinite in the x and y directions, insulated by the xy plane at $z=0$ and in contact with an infinite blood mass at $z=1$ cm (Fig. 6). It can be shown that the governing equation for the extracellular potential ϕ_e in the tissue is given by

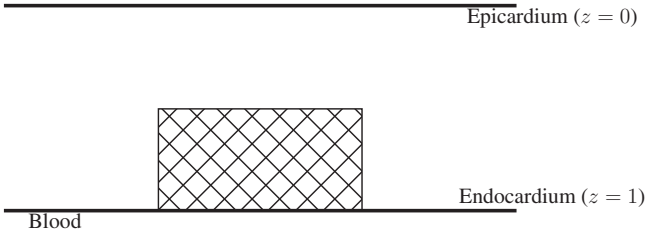

FIG. 6. A slab of cardiac tissue, insulated on the epicardium (at $z=0$) and in contact with a blood mass on the endocardium (at $z=1$). The hatched region represents a region of subendocardial ischemia.

$$\nabla \cdot (\mathbf{M}_i + \mathbf{M}_e) \nabla \phi_e = -\nabla \cdot \mathbf{M}_i \nabla \phi_m \tag{61}$$

with $\phi_m = \phi_i - \phi_e$. The potential in the blood (bath) satisfies Laplace's equation

$$\nabla^2 \phi_b = 0. \tag{62}$$

The boundary conditions required to solve the equations are usually that $\phi_e \to 0$ and $\phi_b \to 0$ as $|x| \to \infty$ and $|y| \to \infty$ and that $\phi_b \to 0$ as $z \to \infty$. It is also required that

$$\frac{\partial \phi_e}{\partial z} = 0 \quad \text{and} \quad \frac{\partial \phi_i}{\partial z} = 0 \quad \text{at } z = 0, \tag{63}$$

$$\phi_e = \phi_b \quad \text{and} \quad \sigma_e^t \frac{\partial \phi_e}{\partial z} = \sigma_b \frac{\partial \phi_b}{\partial z} \quad \text{at } z = 1. \tag{64}$$

(See [6] for complete details of the model.)

In general, to solve the problem, ϕ_m is prescribed and depends on the size and position of the ischemic region in the tissue. Also, it is assumed that

$$\left.\frac{\partial \phi_m}{\partial z}\right|_{z=0} = 0, \qquad \left.\frac{\partial \phi_m}{\partial z}\right|_{z=1} = 0, \qquad \phi_m|_{z=1} = -\Delta\phi$$

where $\Delta\phi$ is the difference in ST segment potentials between the normal and ischemic regions [9]. These conditions imply that the condition

$$\left.\frac{\partial \phi_i}{\partial z}\right|_{z=1} = 0 \tag{65}$$

cannot be satisfied exactly. However, it is generally argued that, if the length constant of the tissue in the transverse direction is small compared to the depth of the tissue, then condition (64) represents an acceptable approximation [6–8].

Following the ideas of Patel and Roth [4], the definitions

$$\phi_m = \phi_m^0 + Ae^{-(1-z)/\lambda} \tag{66}$$

and

$$\phi_e = \phi_e^0 + Be^{-(1-z)/\lambda} \tag{67}$$

make it possible to satisfy the boundary condition (65). However, this choice for the functional representations of ϕ_m and ϕ_e violates the boundary condition $(\partial\phi_i/\partial z)|_{z=0} = 0$.

More appropriate definitions for ϕ_m and ϕ_e should again use an auxiliary function based on the hyperbolic cosine function; that is, write

$$\phi_m = \phi_m^0 + A\frac{\cosh(z/\lambda)}{\cosh(1/\lambda)} \tag{68}$$

and

$$\phi_e = \phi_e^0 + B\frac{\cosh(z/\lambda)}{\cosh(1/\lambda)}, \tag{69}$$

where ϕ_m^0 is a function that captures the general shape of the transmembrane potential distribution, in particular that $(\partial\phi_m^0/\partial z)|_{z=1} = 0$.

Substituting (68) and (69) into Eq. (61) and requiring that $(\partial\phi_i/\partial z)|_{z=1} = 0$, we obtain

$$A = -\lambda \coth(1/\lambda)\frac{\sigma_i^t + \sigma_e^t}{\sigma_e^t}\left.\frac{\partial \phi_e^0}{\partial z}\right|_{z=1}$$

and

$$B = \lambda \coth(1/\lambda)\frac{\sigma_i^t}{\sigma_e^t}\left.\frac{\partial \phi_e^0}{\partial z}\right|_{z=1},$$

where ϕ_e^0 satisfies

$$\nabla \cdot (\mathbf{M}_i + \mathbf{M}_e) \nabla \phi_e^0 = -\nabla \cdot \mathbf{M}_i \nabla \phi_m^0 \tag{70}$$

subject to

$$\frac{\partial \phi_e^0}{\partial z} = 0 \quad \text{at } z = 0, \tag{71}$$

$$\phi_b = \phi_e^0 + \lambda \coth(1/\lambda)\frac{\sigma_i^t}{\sigma_e^t}\frac{\partial \phi_e^0}{\partial z} \quad \text{at } z = 1, \tag{72}$$

$$\sigma_b \frac{\partial \phi_b}{\partial z} = \sigma_e^t\left(1 + \frac{\sigma_i^t}{\sigma_e^t}\right)\frac{\partial \phi_e^0}{\partial z} \quad \text{at } z = 1, \tag{73}$$

with ϕ_b satisfying (62) such that $\phi_b \to 0$ as $z \to \infty$. The same boundary conditions apply to ϕ_e^0 and ϕ_b in the x and y directions as described above.

The problem in terms of ϕ_e^0, ϕ_m^0, and ϕ_b is exactly that described previously [6] and can be solved in an identical manner. There is, however, a slight change to one entry in the coefficient matrix in the one-dimensional numerical scheme used in [6], due to the additional mixed boundary condition at $z=1$, Eq. (72). The extracellular potential ϕ_e can be obtained by calculating ϕ_e^0 via the methods described in [6] and using

$$\phi_e = \phi_e^0 + \lambda \coth(1/\lambda)\left.\frac{\sigma_i^t}{\sigma_e^t}\frac{\partial \phi_e^0}{\partial z}\right|_{z=1}\frac{\cosh(z/\lambda)}{\cosh(1/\lambda)}. \tag{74}$$

Figure 7 shows the epicardial ($z=0$) surface potential distributions, for a 16×16 cm^2 slab of cardiac tissue, 1 cm thick, containing a 4×4 cm^2 region of 50% ischemia, obtained using (a) the method described in [6] and (b) the modified methods described here [Eq. (74)]. The conductivity values used are those given by Clerc [21], and the slab contains no fiber rotation. The main difference between the two figures is the shape of the contour at −0.6 mV. For the solution method described in [6], this particular contour is a single continuous curve [Fig. 7(a)], while the modifications introduced here produce three distinct curves [Fig. 7(b)]. Also, Eq. (74) indicates a slightly higher minimum potential and a slightly higher maximum potential. Interestingly, the solution obtained from Eq. (74) more closely matches a numerical solution for the same problem based on the finite volume method [11].

As a second example, consider the same slab of cardiac tissue, this time with 120° fiber rotation from the epicardium to the endocardium, with the fibers oriented along the x axis on the epicardium. The epicardial potential distributions are shown in Fig. 8, with Fig. 8(a) showing the distribution obtained using the techniques from [6] and Fig. 8(b) showing the distribution from Eq. (74). In this example, the differ-

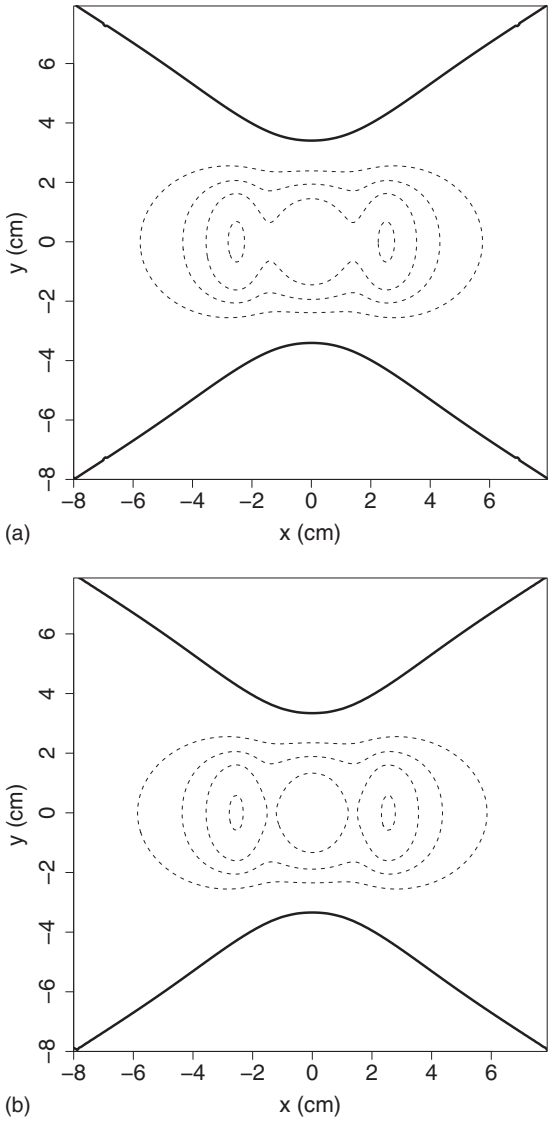

FIG. 7. Epicardial potential distributions on the surface of a slab of cardiac tissue with no fiber rotation. Negative potentials are indicated by dashed lines and the zero of the potential is denoted by the thick solid line. The contour interval is 0.2 mV. (a) shows the solution obtained from [6] (with a minimum potential of −0.8279 mV and a maximum potential of 0.0276 mV) and (b) is the solution obtained using the method described here (with a minimum potential of −0.8205 mV and a maximum potential of 0.0292 mV).

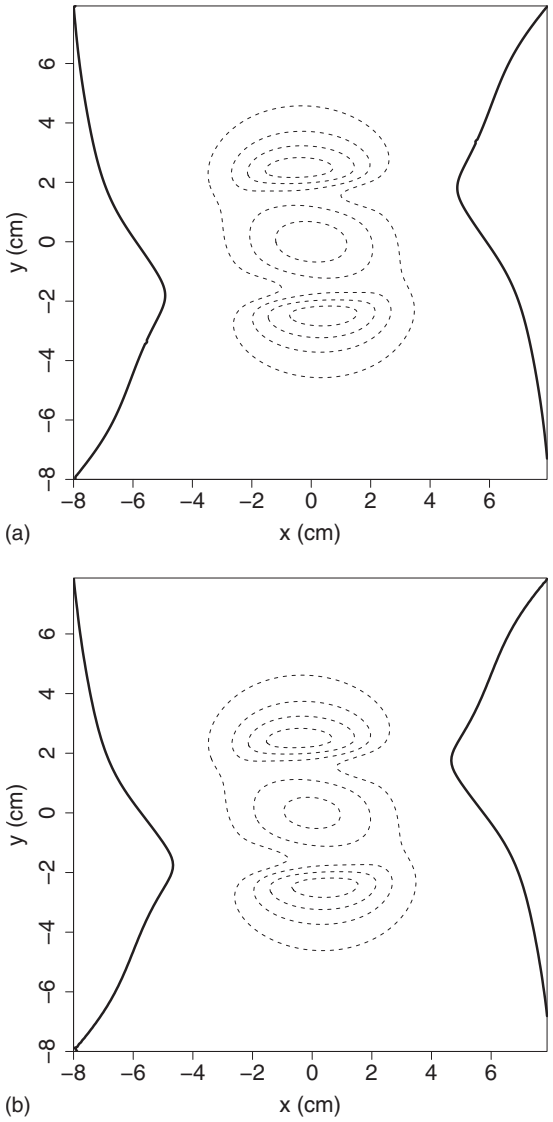

FIG. 8. Epicardial potential distributions on the surface of a slab of cardiac tissue with 120° of fiber rotation. Negative potentials are indicated by dashed lines and the zero of the potential is denoted by the thick solid line. The contour interval is 0.2 mV. (a) is the solution obtained from [6] (with a minimum potential of −0.9149 mV and maximum potential of 0.0099 mV) and (b) is the solution obtained using the method described here (with a minimum potential of −0.9084 mV and a maximum potential of 0.0113 mV).

ences between the two contour plots are very difficult to see with the naked eye. The main distinctions between the two plots are the slight differences between the extremes in the potential values.

Similar results can be achieved when the cylindrical model of the left ventricle is considered [8]. In that case it would be necessary to choose

$$\phi_m = \phi_m^0 + A\frac{I_0((b-r)/\lambda)}{I_0((b-a)/\lambda)},$$

with a similar expression for ϕ_e. Here the auxiliary function is based on I_0, the zero-order modified Bessel function, with a and b representing the inner and outer radii of the ventricular muscle, respectively.

It was mentioned by Patel and Roth [4] that there is a difference in the coefficients obtained by ignoring and then allowing for satisfaction of the boundary condition (10). Using their conductivity data, there is a difference of 17% [4] in the coefficient relating to the bath potential, but there is a difference of only 3% in the coefficient relating to the tissue potential. They claim that the differences may be significant in precise quantitative measurements, but are probably not important for qualitative analysis of an ECG. Figures 7 and 8 show the extent of this difference for the case of subendocardial ischemia during the ST segment. There may be more significant differences in studies of other aspects of the ECG

and perhaps the differences are manifest more strongly in the bath than in the tissue.

VIII. CONCLUSIONS

This paper has presented an analysis of the approximate methods suggested by Patel and Roth [4,5] for solving problems in electrocardiography. It has been shown that their approximation method can be improved for defibrillation problems by consideration of auxiliary functions that are more appropriate to the geometry of the problem under consideration. In the example considered here, use of a modified Bessel function as the auxiliary function gave more accurate solutions to the defibrillation of a thin fiber than use of an exponential function [5].

For electrocardiogram problems, it was shown that choosing auxiliary functions that satisfied all boundary conditions and ensuring that all boundary conditions were satisfied during the solution process provided solutions that were not significantly different from those produced by the original approximate methods [4]. This demonstrates the appropriateness of the original approximations introduced by Patel and Roth.

One interesting result from the analysis performed in this paper was that the approximate method of Patel and Roth [4] is equivalent to an approach published by Roth and Wikswo [19] some 20 years ago. Hence it can be concluded that, for cardiac propagation problems, good approximate solutions to Eqs. (1) and (2) subject to boundary conditions (8)–(10) can be obtained by solving Eqs. (1) and (2) subject to boundary conditions (8) and (33) and assuming that the transmembrane potential does not vary in the direction normal to the fiber direction.

Finally, for problems simulating epicardial potential distributions from subendocardial ischemia during the ST segment, the approximate solutions obtained using the methods described here more closely reproduce the full numerical solution than those published previously [6].

[1] L. Tung, Ph.D. thesis, Massachusetts Institute of Technology, 1978.
[2] I. J. LeGrice, B. H. Smaill, L. Z. Chai, S. G. Edgar, J. B. Gavin, and P. J. Hunter, Am. J. Physiol. **269**, H571 (1995).
[3] O. H. Schmitt, in *Information Processing in the Nervous System*, edited by K. N. Leibovic (Springer, New York, 1969), Chap. 18, pp. 325–331.
[4] S. G. Patel and B. J. Roth, Phys. Rev. E **72**, 051931 (2005).
[5] S. G. Patel and B. J. Roth, Phys. Rev. E **71**, 021908 (2005).
[6] P. R. Johnston, D. Kilpatrick, and C. Y. Li, IEEE Trans. Biomed. Eng. **48**, 1366 (2001).
[7] P. R. Johnston and D. Kilpatrick, IEEE Trans. Biomed. Eng. **50**, 150 (2003).
[8] P. R. Johnston, Math. Biosci. **186**, 43 (2003).
[9] P. R. Johnston, Math. Biosci. **198**, 97 (2005).
[10] M. C. MacLachlan, J. Sundnes, O. Skavhaug, M. Lysaker, B. F. Nielsen, and A. Tveito, Math. Biosci. **210**, 238 (2007).
[11] R. C. Penland, D. M. Harrild, and C. S. Henriquez, Comput. Visualization Sci. **4**, 215 (2002).
[12] M. Trew, I. Le Grice, B. Smaill, and A. Pullan, Ann. Biomed. Eng. **33**, 590 (2005).
[13] J. Sundnes, G. T. Lines, and A. Tveito, Math. Biosci. **194**, 233 (2005).
[14] B. M. Johnston, P. R. Johnston, and D. Kilpatrick, Math. Biosci. **202**, 288 (2006).
[15] B. M. Johnston, P. R. Johnston, and D. Kilpatrick, Comput. Methods Biomech. Biomed. Eng. **11**, 223 (2008).
[16] B. J. Roth, IEEE Trans. Biomed. Eng. **44**, 326 (1997).
[17] B. J. Roth and D. Langrill-Beaudoin, Phys. Rev. E **67**, 051925 (2003).
[18] J. C. Clements and B. M. Horáček, IEEE Trans. Biomed. Eng. **52**, 1784 (2005).
[19] B. J. Roth and J. P. Wikswo, Jr., IEEE Trans. Biomed. Eng. **BME-33**, 467 (1986).
[20] W. Krassowska and J. Neu, IEEE Trans. Biomed. Eng. **41**, 143 (1994).
[21] L. Clerc, J. Physiol. (London) **255**, 335 (1976).